

Improving Wind Resistance Performance of Cascaded PID Controlled Quadcopters using Residual Reinforcement Learning

Yu Ishihara¹, Yuichi Hazama², Kousuke Suzuki², Jerry Jun Yokono¹, Kohtaro Sabe², and Kenta Kawamoto^{1,3}

Abstract—Wind resistance control is an essential feature for quadcopters to maintain their position to avoid deviation from target position and prevent collisions with obstacles. Conventionally, cascaded PID controller is used for the control of quadcopters for its simplicity and ease of tuning its parameters. However, it is weak against wind disturbances and the quadcopter can easily deviate from target position. In this work, we propose a residual reinforcement learning based approach to build a wind resistance controller of a quadcopter. By learning only the residual that compensates the disturbance, we can continue using the cascaded PID controller as the base controller of the quadcopter but improve its performance against wind disturbances. To avoid unexpected crashes and destructions of quadcopters, our method does not require real hardware for data collection and training. The controller is trained only on a simulator and directly applied to the target hardware without extra finetuning process. We demonstrate the effectiveness of our approach through various experiments including an experiment in an outdoor scene with wind speed greater than 13 m/s. Despite its simplicity, our controller reduces the position deviation by approximately 50 % compared to the quadcopter controlled with the conventional cascaded PID controller. Furthermore, trained controller is robust and preserves its performance even though the quadcopter’s mass and propeller’s lift coefficient is changed between 50 % to 150 % from original training time.

I. INTRODUCTION

Quadcopters are coming to be used for a variety of applications such as delivery, filming, and surveying. These applications often require a quadcopter to be used in an outdoor scene where an unpredictable wind disturbances exist. A quadcopter flying outdoors may collide with nearby obstacles or deviate from target position when an unexpected gust of wind blows. Therefore, there is a high demand on quadcopters with a controller that can stabilize and maintain its position and orientation under wind disturbances.

Model-free cascaded PID controllers are widely used as a controller for quadcopters because of its simplicity to implement and to tune their parameters [1]. However, this controller is prone to wind disturbances due to its controller design[2], [3]. Cascaded PID controller needs to wait for the convergence of subsequent layers to reflect the higher layers control input (e.g. position control input). Hence, the controller delays in react and deviates from target position when sudden external disturbances occur. Existing research approaches this issue by replacing the cascaded

PID controller. However, these approaches require to model the system’s dynamics [4], [5], [6], [7], [2] or learn a controller from data [8] for different quadcopters. Therefore, the simplicity of cascaded PID controller is lost and makes it difficult to apply the controller on a variety of quadcopters. Especially in industrial applications, it is often preferred to keep the simplicity of PID controller but to make the system robust against wind disturbances.

In this work, we investigate for a method to build a robust controller against wind disturbances using cascaded PID controller as a base controller of the system. Specifically, we apply residual reinforcement learning [9] and make a policy model learn only the residual of control input that compensates the wind disturbances. To avoid unexpected crashes and destructions of a quadcopter, we train the controller solely on a simulator and directly apply the trained controller to the target hardware without extra fine tuning in a real environment. The training only requires approximately 12 hours wall-clock time. We will demonstrate the effectiveness of our approach through various simulations and experiments including an experiment in an outdoor scene with wind speed greater than 13 m/s. Despite its simplicity, the proposed method reduces the position deviation by approximately 50 % compared to the conventional cascaded PID controller. It also preserves its performance even when the quadcopter’s parameter (mass and propeller’s lift-coefficient) changes between 50 % to 150 % from original training time.

The contributions of this paper are as follows.

- Proposal of wind resistance controller for quadcopters trained with residual reinforcement learning to enable cascaded PID controller resistant to wind disturbances.
- Demonstration of the effectiveness of the proposed controller through simulations and experiments including an experiment in an outdoor environment with wind speed greater than 13 m/s.

II. RELATED WORK

A. Wind Resistance Control of Quadcopters

Wind resistant controller for quadcopters has been an active area of research for their high demands on many commercial applications. Previous approaches estimate the wind disturbance [4], [6], [7] or apply robust control method [5], [2] to make the quadcopter’s controller resistant against wind disturbances. To enable such control, the quadcopter’s dynamics is estimated or determined in advance [4], [5], [6], [7] and control algorithms such as MPC [4], [6], [7], H_∞ [5], or L_1 adaptive control [2] are applied to control

¹Sony Group Corporation, 1-7-1 Konan Minato-ku, Tokyo, 108-0075, Japan. Corresponding author: yu.ishihara@sony.com

²Aerosense Inc., 5-41-10 Koishikawa, Bunkyo-ku, Tokyo, 112-0002, Japan

³Sony Research Inc., 1-7-1 Konan Minato-ku, Tokyo, 108-0075, Japan

the quadcopter under wind disturbances. These approaches require identifying the quadcopter’s system and customizing their control parameters for each quadcopter. Hence, they are difficult to apply in case the system’s dynamics changes drastically during the operation (e.g. package delivery with a quadcopter). Considering varieties of applications and quadcopters, it is preferred to build a controller that can be used even though a quadcopter’s system changes. In this work, we incorporate residual reinforcement learning approach and build a wind resistant controller for quadcopters. We will show that the learned controller can control the quadcopter even when the quadcopter’s parameter (mass and propeller’s lift-coefficient) changes between 50 % to 150 % from original training time.

B. Reinforcement Learning for Robotic Applications

Recently, reinforcement learning [10] has been used to train a wide variety of robotic applications including quadcopters [11], [12], [13], [14], [15]. Since reinforcement learning enables to learn and optimize robot’s behavior without knowing the underlying dynamics of the system, it has been applied to applications that conventional model-based methods are difficult to apply. Taylor et al. trained a bipedal robot to learn its locomotion from human motion capture data [11]. Li et al. also trained a bipedal robot and realized a robust controller compared to conventional model-based controller that performs a set of diverse and dynamic behaviors of bipedal robots [12]. Miki et al. applied reinforcement learning to navigate a quadrupedal robot on different types of terrains that their surface characteristics are difficult to model [13]. Reinforcement learning is also used for manipulators to learn grasping objects in a cluttered environment [14]. Furthermore, Vankadari et al. trained a controller for autonomous landing of a quadcopter using reinforcement learning [15]. In this paper, we will apply reinforcement learning to learn a wind resistant controller for quadcopters. Since wind disturbances are difficult to model and predict in practice, reinforcement learning was expected as a solution to realize such a controller. We will demonstrate that the trained controller enables to cancel wind disturbances and improve the quadcopter’s performance compared to conventional cascaded PID-based controller.

III. PRELIMINARIES

We train our controller considering the problem as a standard reinforcement learning problem [10]. Reinforcement learning is defined as a policy search in an environment modeled as a Markov decision process, defined by a tuple $(\mathcal{S}, \mathcal{A}, \rho_0, p, r)$. Where \mathcal{S} , \mathcal{A} , ρ_0 , p , r denote the state space, action space, initial state probability, transition probability, and reward function of the environment. The objective of reinforcement learning is to find an optimal policy π^* that maximizes the following expected sum of discounted rewards

$$\pi^* = \arg \max_{\pi} \mathbb{E}_{s_0 \sim \rho_0, s_t > 0 \sim p, a_t \sim \pi} \left[\sum_{t=0}^{\infty} \gamma^t r(s_t, a_t) \right]. \quad (1)$$

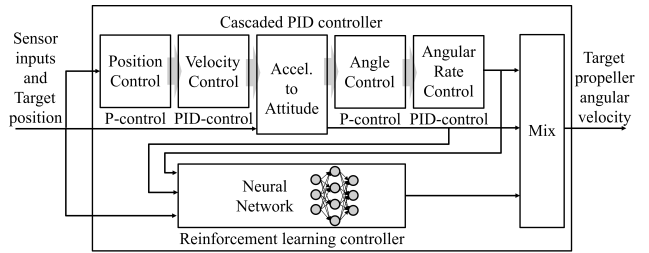


Fig. 1: Architecture of proposed controller. PID controller’s running frequency is between 100 Hz to 1000 Hz (Position control is around 100 Hz but angular rate control is around 1000 Hz). Reinforcement learning controller operates at 10 Hz.

Here, $\gamma \in [0, 1)$ is the discount factor, $s_t \in \mathcal{S}$ and $a_t \in \mathcal{A}$ represents the state and action at time t . In this work, we used Soft Actor-Critic (SAC) [16], [17] as the reinforcement learning algorithm to train the policy π . In SAC, the policy is trained using a reward r_{target} with entropy bonus defined as follows:

$$r(s_t, a_t) \triangleq r_{\text{target}}(s_t, a_t) + \alpha \mathcal{H}(\pi(\cdot|s_t)). \quad (2)$$

$\mathcal{H}(\pi(\cdot|s_t))$ denotes the entropy of the policy and α is a trade-off coefficient. We used SAC because it is known to be robust and sample efficient for robotic tasks [17]. Furthermore, to take advantage of conventional cascaded PID controller, we incorporate the idea of residual reinforcement learning [9]. Our policy π computes action a at each timestep as:

$$a = a_{\text{PID}} + a_{\text{RL}}. \quad (3)$$

a_{PID} is the output of cascaded PID controller and a_{RL} is the action computed using parameterized policy π_{θ} trained with SAC. θ is the parameter of the training policy. Residual reinforcement learning enables the policy π_{θ} to focus on learning to cancel external disturbances and avoids learning to fly the quadcopter from scratch. Therefore, we expected that the training gets much easier and the training time reduces compared to training a policy from scratch.

IV. METHOD

Fig. 1 shows the overview of the proposed controller. As mentioned in previous section, the quadcopter’s controller consists of a cascaded PID controller and a neural network-based controller which is trained using reinforcement learning algorithm. Two controllers run in parallel and their output is mixed to compute the target angular velocity of each propeller. In this work, we made use of cascaded PID controller also used in PX4 [1] as baseline controller. In the following subsections, we will describe the design and the training method of the reinforcement learning controller in detail.

A. Network Model and Controller Design

We designed two neural network models π_{θ} and Q_{ψ} to train the reinforcement learning controller. θ and ψ denotes the parameter of each neural network. π_{θ} corresponds to the

TABLE I: Network structure of π_θ .

Input layer	state input (68 dim)
Middle layer 1	Fully-connected followed by relu (30 dim)
Middle layer 2	Fully-connected followed by relu (20 dim)
Middle layer 3	Fully-connected followed by relu (5 dim)
Output layer	Gaussian mean (4 dim) and variance (4 dim)

 TABLE II: Network structure of Q_ψ .

Input layer	state and action inputs (68+4 dim)
Middle layer 1	Fully-connected followed by relu (400 dim)
Middle layer 2	Fully-connected followed by relu (200 dim)
Middle layer 3	Fully-connected followed by relu (100 dim)
Output layer	Q-value (1 dim)

actor and Q_ψ is the critic used in SAC algorithm. Q_ψ is only used during the training phase to update the parameter of controller π_θ with SAC. Table I and Table II shows the structure of both networks. π_θ is a small neural network which consists of four fully-connected layers. We selected the number of intermediate neurons to enable running the network on quadcopter at 10 Hz. State input is a 68 dimensional vector which consists of following features:

- history of relative position to target (3 dim \times 3 steps)
- history of quadcopter's velocity (3 dim \times 3 steps)
- history of relative angle to target (3 dim \times 3 steps)
- history of quadcopter's angular velocity (3 dim \times 3 steps)
- history of PID-controller's output (4 dim \times 3 steps)
- history of RL-controller's output (4 dim \times 5 steps)

Here, 1 step corresponds to 0.1 s. Final layer is split into two and used as the mean and the variance of a Gaussian distribution. Action $a_{\text{RL}} = (F_{\text{thrust}}^{\text{RL}}, T_{\text{roll}}^{\text{RL}}, T_{\text{pitch}}^{\text{RL}}, T_{\text{yaw}}^{\text{RL}})^T$ is a four dimensional vector that represents the residual of thrust and roll, pitch, yaw torques and is computed as follows.

$$a_{\pi_\theta} = \begin{cases} \sim \mathcal{N}(\mu_\theta, \sigma_\theta) & \text{(Training)} \\ \mu_\theta & \text{(Testing)} \end{cases} \quad (4)$$

$$a_{\hat{\text{RL}}} = \tanh(a_{\pi_\theta}) \quad (5)$$

μ_θ and σ_θ denotes the mean and the standard deviation of the Gaussian distribution computed with π_θ . $a_{\hat{\text{RL}}}$ is combined with PID-controller's output a_{PID} as follows.

$$a_{\text{RL}}^{\text{shifted}} = \frac{1}{2}(a_{\hat{\text{RL}}} + 1) \times \beta - \epsilon \quad (6)$$

$$a_{\text{RL}}^{\text{scaled}} = a_{\text{RL}}^{\text{shifted}} \odot (a_{\text{RL}}^{\text{max}} - a_{\text{RL}}^{\text{min}}) + a_{\text{RL}}^{\text{min}} \quad (7)$$

$$a_{\text{RL}} = \text{clip}(a_{\text{RL}}^{\text{scaled}}, a_{\text{RL}}^{\text{min}}, a_{\text{RL}}^{\text{max}}) \quad (8)$$

$$a = a_{\text{PID}} + a_{\text{RL}} \quad (9)$$

Equation (6) shifts the output squashed with tanh in (5) to the range of $[-\epsilon, \beta - \epsilon]$. This shift operation enables the reinforcement learning controller to output values between $[a_{\text{RL}}^{\text{min}}, a_{\text{RL}}^{\text{max}}]$ using (7) and (8). Without (6), values near $a_{\text{RL}}^{\text{min}}$ and $a_{\text{RL}}^{\text{max}}$ are not computed because it is computationally infeasible for tanh to output values near -1 and 1. \odot denotes the hadamard product. In this work, we set $\beta = 1.2$, $\epsilon = 0.1$, $a_{\text{RL}}^{\text{max}} = (0.25, 0.1, 0.1, 0.1)^T$, and $a_{\text{RL}}^{\text{min}} = -a_{\text{RL}}^{\text{max}}$. Finally, we compute propeller's angular velocity using the following

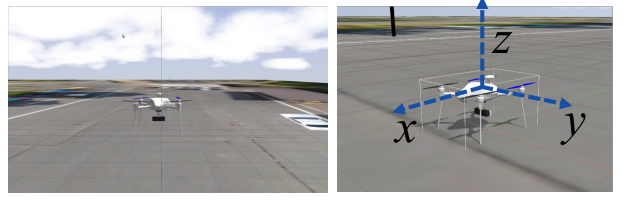


Fig. 2: Simulation environment.

relationship between $a = (F_{\text{thrust}}, T_{\text{roll}}, T_{\text{pitch}}, T_{\text{yaw}})^T$ in (9) and propeller's angular velocity $\omega = (\omega_0, \omega_1, \omega_2, \omega_3)^T$.

$$\begin{pmatrix} F_{\text{thrust}} \\ T_{\text{roll}} \\ T_{\text{pitch}} \\ T_{\text{yaw}} \end{pmatrix} = \begin{pmatrix} 1 & 1 & 1 & 1 \\ -c & c & c & -c \\ c & -c & c & -c \\ 1 & 1 & -1 & -1 \end{pmatrix} \begin{pmatrix} \omega_0^2 \\ \omega_1^2 \\ \omega_2^2 \\ \omega_3^2 \end{pmatrix}, \quad c = \frac{1}{\sqrt{2}} \quad (10)$$

B. Training Method

We trained the presented networks using SAC in a simulation environment shown in Fig. 2. This simulation environment was built on top of Gazebo physics simulator [18]. We used PX4 [1] as the base flight controller of our quadcopter [19] model in the simulation. We trained the controller using only a single quadcopter model. However, we will show in the evaluation section that the trained controller also works on quadcopters with mass and lift coefficient parameters different from original model. During the training, simulated wind, between 15 m/s to 25 m/s, blows from 26 different directions¹ at random. The wind speed linearly increases from zero to selected wind speed in 1 s and keeps blowing at selected speed for 3 s. We expected that, by training the quadcopter with different wind speed, the trained controller gets robust not only against wind disturbances but also against changes in quadcopter's parameters (mass and lift coefficient). This is because the controller trained to compensate for forces of different magnitudes should also compensate for changes in the forces on the quadcopter due to differences in mass and lift-coefficient.

We designed the following reward function to train the network

$$r = w_{\text{pos}}r_{\text{pos}} + w_{\text{rp}}r_{\text{rp}} + w_{\text{yt}}r_{\text{yt}}. \quad (11)$$

w_{pos} , w_{rp} , and w_{yt} are the weights of each term and r_{pos} , r_{rp} , and r_{yt} are described as follows:

$$r_{\text{pos}} = \min(-\Delta_t + \Delta_{t-1}, 0), \quad (12)$$

$$\text{where } \Delta_t = \sqrt{\Delta x_t^2 + \Delta y_t^2 + \Delta z_t^2}$$

$$r_{\text{rp}} = -(|T_{\text{roll},t} - T_{\text{roll},t-1}| + |T_{\text{pitch},t} - T_{\text{pitch},t-1}|) \quad (13)$$

$$r_{\text{yt}} = -(|T_{\text{yaw},t} - T_{\text{yaw},t-1}| + |F_{\text{thrust},t} - F_{\text{thrust},t-1}|). \quad (14)$$

Δx_t , Δy_t , and Δz_t denotes the relative distance to the target position for each axis at time t . Hence, r_{pos} penalizes the policy when the quadcopter diverges from the target position

¹ $26 = 3^3 - 1$ comes from the possible combinations of +, -, 0 for each axis. (+, 0, 0), (+, +, 0), ..., (+, +, +), (-, 0, 0), ..., (-, -, -)

compared to previous timestep. r_{tp} and r_{yt} are designed for similar purpose to penalize rapid changes in the output of policy π_{θ} . We weighted (13) and (14) separately because we assumed that roll and pitch angle affect quadcopter’s position greater than yaw angle and thrust. We set the weights to $w_{\text{pos}} = 1$, $w_{\text{rp}} = 2.5 \times 10^{-2}$, and $w_{\text{yt}} = 5 \times 10^{-3}$.

We set the discount factor γ to 0.95, batch size to 128, and target network update coefficient τ used in SAC to 1.0×10^{-4} . Network parameters were updated using Adam [20] with learning rate of 2.0×10^{-4} . During the training, we applied uniformly sampled noise between $[-1, 1)$ to each state element in batch to imitate the sensor noise on real quadcopters. When applying the noise, we scaled the sampled noise by 0.1 for relative position, by 0.5 for velocity, by 0.05 for relative angle, by 1.25 for angular velocity, and by 0.1 for PID-controller’s output. We did not append this noise to RL-controller’s output. We ran the training until average reward received by the quadcopter converges and used the best parameter learned in the evaluation. The training took approximately 12 hours (wall-clock time).

V. SIMULATION

A. Performance Evaluation

We evaluated the performance of the proposed controller in the simulation environment presented in previous section (See Fig. 2). During the evaluation, simulated gust of wind of 20 m/s blows from 26 different directions as in previous section to check the performance of trained controller. For each wind direction, the wind blows once for 30 steps (i.e. 3 s). There are 70 steps (i.e. 7 s) of interval until the wind blows from another direction. In the evaluation, we used the conventional cascaded PID controller as a baseline method and compared with the proposed controller. In prior to the evaluation, the PID parameters were manually tuned using real quadcopter (AS-MC03-W2 [21], see Appendix I), and selected the best performing PID parameters under wind disturbances for the comparison. We used this PID parameters for both evaluation and training of the proposed controller.

Fig. 3 shows the position history of the quadcopter during the simulation. Each of the 26 different positional peak in the figure corresponds to the number of wind directions blown in the evaluation. Proposed controller succeeds in reducing the deviation in all wind directions by approximately 50% compared to the baseline cascaded PID controller. The overall result is shown in Table III. From Table III, we can also verify that the proposed controller succeeds in reducing the deviation from target position. The improvement in standard deviation of overall positional error was around 45% to 63% in our evaluation.

B. Robustness Evaluation

We checked the robustness of proposed controller against the changes in quadcopter’s mass and propeller’s lift coefficient. We evaluated the robustness against these changes because quadcopter’s mass may change dynamically when it loads or unloads additional payloads and propeller’s lift

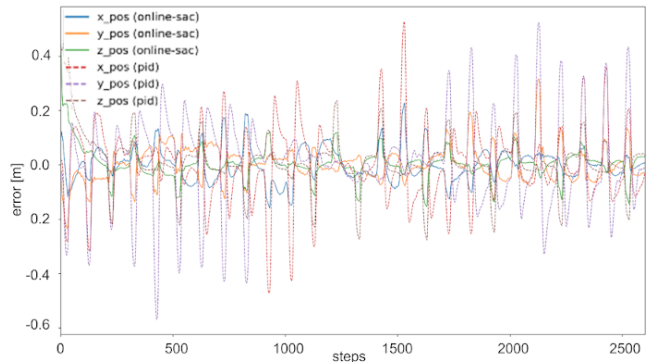


Fig. 3: Positional error of quadcopter during evaluation (Dotted lines: conventional cascaded PID-controller, solid lines: PID+reinforcement learning controller (Proposed)). Proposed controller reduces the deviation by approximately 50% compared to PID-only controller.

TABLE III: Positional error of each controller.

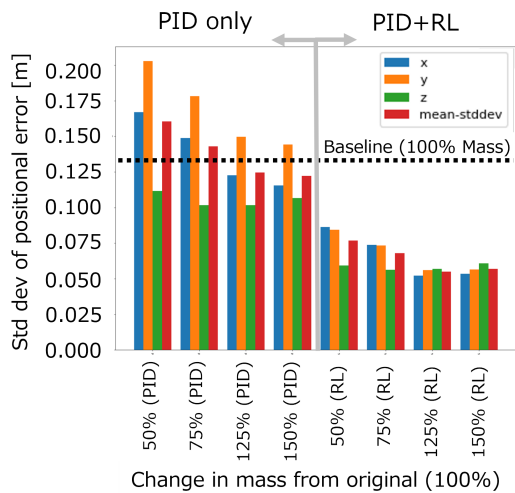
Axis	Cascaded PID [m] (mean \pm std dev.)	Proposed [m] (mean \pm std dev.)	Improvement
x	0.003 \pm 0.132	0.002 \pm 0.060	55 %
y	0.002 \pm 0.166	0.002 \pm 0.063	63 %
z	0.014 \pm 0.099	0.006 \pm 0.055	45 %

coefficient is affected by the air density of the environment. In addition, these parameters change depending on the hardware. We used the same controller and same experiment procedure used in the performance evaluation for this robustness evaluation. During the evaluation, we fixed the lift coefficient to original value and changed the mass of the quadcopter and vice versa to check the robustness of the controller against each parameter.

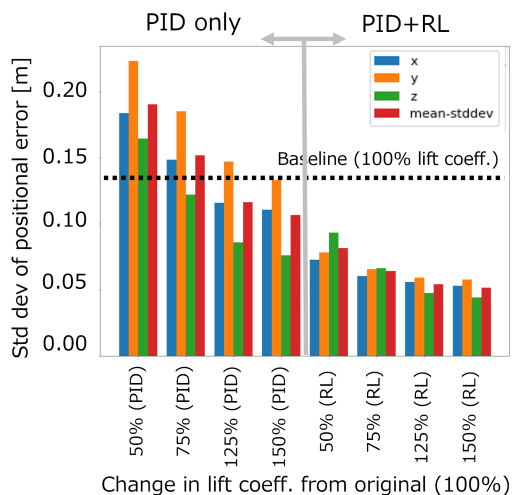
Fig. 4a and Fig. 4b show the standard deviation of the quadcopter’s position against the changes in its parameters. Dotted line shows the average standard deviation of the quadcopter with original mass and lift coefficient controlled using conventional cascaded PID-controller. From the figure, we can confirm that the proposed controller preserves its performance even though the quadcopter’s parameter changes from original training time. The proposed controller succeeded in reducing the deviation from target position by approximately 40% to 60% compared to the conventional cascaded PID controller. Even though the quadcopter’s mass or propeller’s lift coefficient changes drastically (in the range of 50% to 150%), the proposed controller performs better than manually tuned PID-controller on original quadcopter. See also Appendix II for the performance of proposed controller on other combinations of mass and lift coefficient values.

VI. OUTDOOR EXPERIMENTS

We evaluated the performance of proposed controller using a real quadcopter in an outdoor environment shown in Fig. 5. The evaluation was performed in two different conditions: low wind speed (less than 7 m/s) condition and high wind speed (greater than 13 m/s) condition. We evaluated the same



(a) Mass of the quadcopter vs positional error



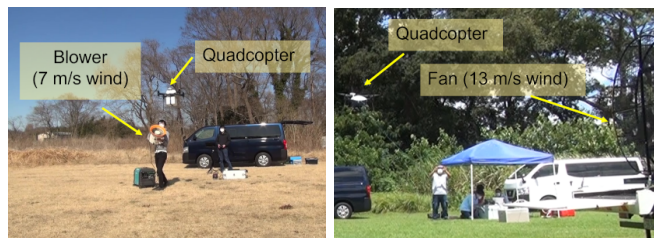
(b) Propeller's lift coefficient vs positional error

Fig. 4: Relationship between the positional error of quadcopter and changes in quadcopter's parameters. Dotted line shows the baseline PID controller's performance. Reinforcement learning controller preserves its performance even though the parameters change.

controller used in the simulation without extra fine tuning for this experiment.

A. Performance under Low Wind Speed Condition

Fig. 6 and Fig. 7 show the behavior of the quadcopter during the experiment. For this experiment, we used a quadcopter with an extra payload of 1 kg. See Appendix I for the details of the hardware used. In the experiment, we manually hit the wind using a blower for around 5s-10s several times and checked the behavior of the quadcopter. From Fig. 6, we can confirm that the conventional cascaded PID controller easily deviates from the target position when the wind from the blower hits the quadcopter. Conversely, from Fig. 7, we can verify that the proposed controller succeeds in maintaining its position. Fig. 8 shows the full



(a) Low wind speed

(b) High wind speed

Fig. 5: Outdoor experimental environment

TABLE IV: Average and maximum absolute positional error of quadcopter under low wind speed condition.

	Cascaded PID	Proposed	Improvement
Average [m] (mean±std dev.)	0.29 ± 0.17	0.17 ± 0.09	mean: 41 % std dev.: 53 %
Maximum [m]	0.93	0.48	52 %

history of absolute positional error of the quadcopter during this experiment. We hit the wind to the quadcopter three times each. From the figure, we can also verify that the proposed controller is effective in stabilizing the quadcopter around target position. Table IV shows the overall result of the experiment. The mean and standard deviation in the table shows the average deviation in the xy-coordinate. We removed the z-coordinate from the calculation because we used a barometer-based sensor to compute the quadcopter's position in the z-coordinate. Barometer-based localization was inaccurate when the gust of wind hit the quadcopter. From Table IV, we can confirm that the deviation from target position using the proposed controller is smaller than the conventional cascaded PID controller. Our controller succeeded in reducing the deviation by 41 % on average and by 52 % on maximum position compared to the conventional cascaded PID controller.

B. Performance under High Wind Speed Condition

In this experiment, we used a large fan shown in Fig. 5b to imitate a scene with complex wind gust condition. We used a different quadcopter from previous evaluation to check the robustness of our controller. The quadcopter has different shapes and is connected by a wire for electric power supply (i.e. extra load is applied depending on the altitude of the quadcopter). See also Appendix I for the details of the hardware used. The fan shown in Fig. 5b continuously sends wind of approximately 13m/s to the quadcopter during the experiment. We limited the wind speed to 13 m/s considering the safety of the quadcopter during the experiment. According to the Beaufort scale [22], wind speed greater than 13 m/s is classified as an environment where people feel inconvenience walking against the wind. The wind gust is highly difficult to predict because the fan generates a complex current of air around the quadcopter. During the experiment, we monitored the source wind speed and kept the source wind speed greater than 13 m/s.

Fig. 9 shows the history of quadcopter's positional error during the experiment. From the figure, we can confirm that

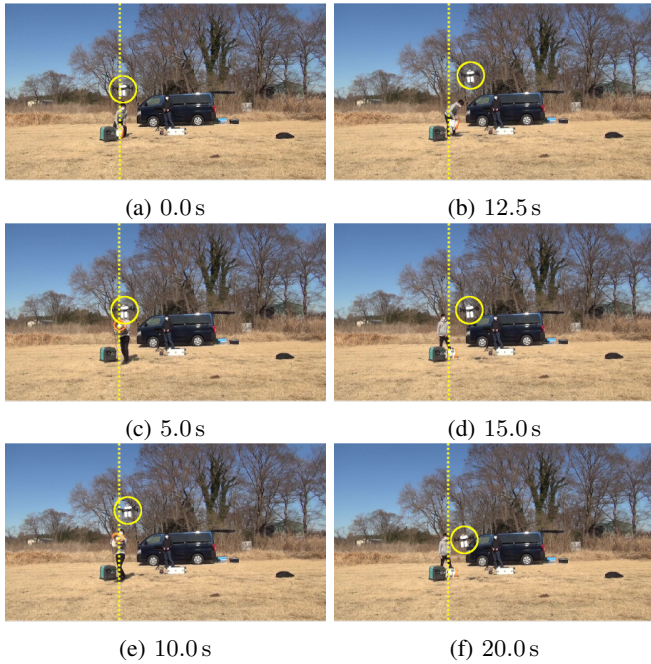


Fig. 6: Snapshots of the quadcopter with cascaded PID-controller under low wind speed Condition.

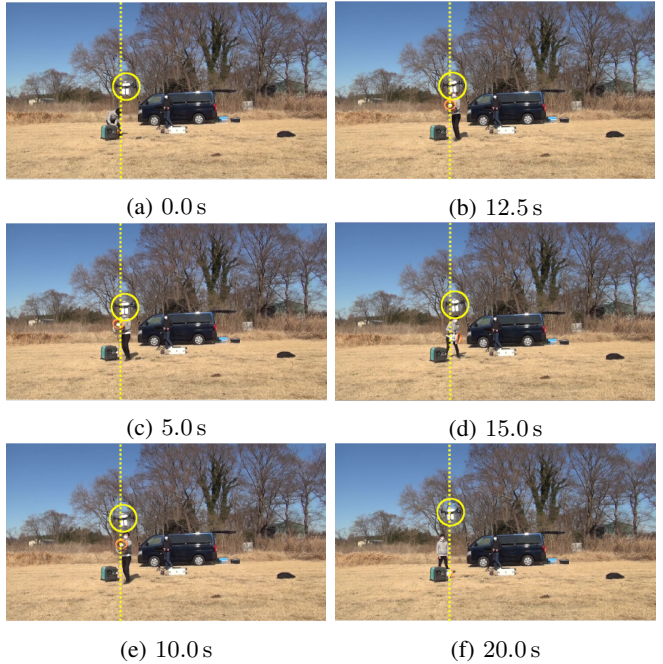


Fig. 7: Snapshots of the quadcopter with proposed controller under low wind speed condition.

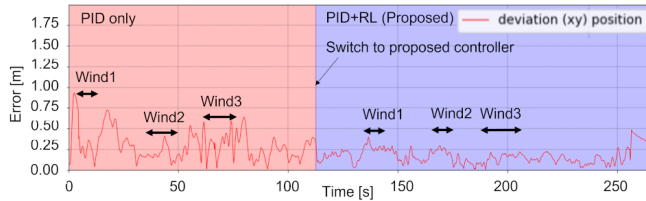
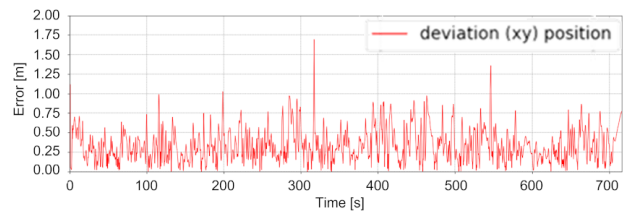


Fig. 8: History of absolute positional error of the quadcopter during low wind speed experiment. Left and right arrows show the wind blowing times.

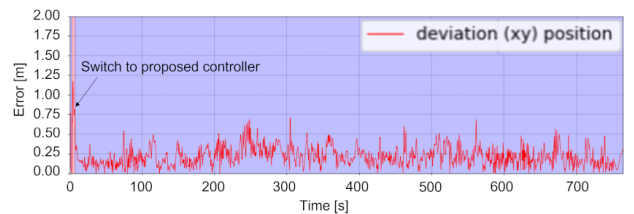
TABLE V: Average and maximum absolute positional error of quadcopter under high wind speed condition.

	Cascaded PID	Proposed	Improvement
Average [m] (mean \pm std dev.)	0.34 ± 0.20	0.22 ± 0.13	mean: 35 % std dev.: 33 %
Maximum [m]	1.69	0.78	53 %

the proposed controller significantly reduces the deviation from target position compared to the conventional cascaded PID controller. Conventional controller deviated from target position by more than 1 m several times during the experiment. In contrast, proposed controller successfully stabilized the quadcopter and prevented the quadcopter largely deviating from target position. The maximum deviation of proposed controller was approximately 0.78 m. Table V shows the overall result of the experiment. From the table, we can also verify that the proposed controller improves the stabilization performance of the quadcopter. Proposed controller reduces the deviation from target position by 35 % on average and by 53 % on maximum position.



(a) Cascaded PID controller



(b) Proposed controller

Fig. 9: History of absolute positional error of the quadcopter during high wind speed experiment. The wind was blowing constantly throughout the experiment.

VII. CONCLUSION AND FUTURE WORK

We presented a residual reinforcement learning approach to build a wind resistance controller for quadcopters. Proposed method uses conventional cascaded PID-controller as a base controller and learns the residual input that compensates the wind disturbances. The residual controller can be trained using only a simulator and no extra finetuning is necessary to run on a real hardware. We evaluated the proposed controller's performance in both simulation and experiment in a real environment. The trained controller reduces the



(a) AS-MC03-T

(b) AS-MC03-W2

Fig. 10: Quadcopters used in each experiment. (a) used in low wind speed experiment. (b) used in high wind speed experiment.

[!tb]

TABLE VI: Hardware Specification of AS-MC03-T.

Size (length×width×height)	943 mm×943 mm×450 mm
Weight	3.53 kg
Max payload	3 kg
Max velocity	54 km/h
Shipping box size	186 mm×258 mm×155 mm
Shipping box weight	267 g

TABLE VII: Hardware Specification of AS-MC03-W2.

Size (length×width×height)	943 mm×943 mm×450 mm
Weight (Quadcopter + Camera)	5.12 kg (4.14 kg + 0.98 kg)
Maximum payload	3 kg
Maximum velocity	18 km/h

positional deviation by approximately 50% compared to conventional cascaded PID controller. In addition, the trained controller preserves its performance even though the quadcopter's parameters (mass and propeller's lift coefficient) have changed from original training time in the range of 50% to 150%.

We demonstrated that our controller works not only in simulation but also on real hardware. During the experiment, we could not observe the system getting unstable. However, the stability of the proposed system is not guaranteed theoretically and may get unstable in a special situation. Investigating the stability of the system could be a future work of this study.

APPENDIX I

HARDWARE SPECIFICATION

Fig. 10 shows the quadcopter used in each real environment experiment [21], [19]. See Table VI and Table VII for the specification of each quadcopter. Please note that AS-MC03-T is a wireless quadcopter and AS-MC03-W2 is a wired quadcopter. Therefore a extra load is applied to AS-MC03-W2 during the flight depending on the flight altitude.

APPENDIX II

EXTRA SIMULATION RESULTS

Matrix on Fig. 11 shows the performance improvement of the proposed controller against the conventional cascaded PID-controller run on original quadcopter (100% mass and

Lift coefficient	150%	X: 46% Y: 57% Z: 52%	X: 51% Y: 62% Z: 57%	X: 60% Y: 63% Z: 56%	X: 64% Y: 69% Z: 59%	X: 62% Y: 68% Z: 58%
	125%	X: 45% Y: 55% Z: 45%	X: 51% Y: 60% Z: 51%	X: 58% Y: 63% Z: 52%	X: 65% Y: 66% Z: 52%	X: 61% Y: 67% Z: 49%
	100%	X: 35% Y: 48% Z: 40%	X: 44% Y: 54% Z: 43%	X: 51% Y: 58% Z: 75%	X: 61% Y: 65% Z: 43%	X: 60% Y: 65% Z: 39%
	75%	X: 33% Y: 42% Z: 29%	X: 43% Y: 52% Z: 32%	X: 54% Y: 59% Z: 33%	X: 59% Y: 60% Z: 31%	X: 58% Y: 56% Z: 20%
	50%	X: -6% Y: 21% Z: 6%	X: 39% Y: 45% Z: 14%	X: 45% Y: 51% Z: 7%	X: 22% Y: 14% Z: -20%	X
		50%	75%	100%	125%	150%
		Mass				

Fig. 11: Improvement in wind resistance performance along each axis. For x and y axis, the more the mass and lift coefficient, the more improvement in performance. For z axis, original weight and lift coefficient performs best. Box with a cross denotes the parameter that failed to fly.

lift coefficient). We can confirm that the proposed controller improves the control performance in most of the combinations by 50% or greater.

ACKNOWLEDGMENT

We would like to express our special thanks to Hiroataka Suzuki, Shunichi Sekiguchi, and Tokuhiko Nishikawa at Sony Group Corporation for their helpful feedback on the early draft of this manuscript and Aerosense Inc. members for their kind support on conducting the experiments.

REFERENCES

- [1] L. Meier, D. Honegger, and M. Pollefeys, "Px4: A node-based multithreaded open source robotics framework for deeply embedded platforms," in *2015 IEEE International Conference on Robotics and Automation (ICRA)*, 2015, pp. 6235–6240.
- [2] R. A. Suárez Fernández, S. Dominguez, and P. Campoy, "L1 adaptive control for wind gust rejection in quad-rotor uav wind turbine inspection," in *2017 International Conference on Unmanned Aircraft Systems (ICUAS)*, 2017, pp. 1840–1849.
- [3] D. Mellinger, N. Michael, and V. Kumar, "Trajectory generation and control for precise aggressive maneuvers with quadrotors," *The International Journal of Robotics Research*, vol. 31, no. 5, pp. 664–674, 2012. [Online]. Available: <https://doi.org/10.1177/0278364911434236>
- [4] J. X. J. Bannwarth, Z. J. Chen, K. A. Stol, and B. A. MacDonald, "Disturbance accommodation control for wind rejection of a quadcopter," in *2016 International Conference on Unmanned Aircraft Systems (ICUAS)*, 2016, pp. 695–701.
- [5] C. MASSÉ, O. GOUGEON, D.-T. NGUYEN, and D. SAUSSIÉ, "Modeling and control of a quadcopter flying in a wind field: A comparison between lqr and structured H_∞ control techniques," in *2018 International Conference on Unmanned Aircraft Systems (ICUAS)*, 2018, pp. 1408–1417.
- [6] N. Schmid, J. Gruner, H. S. Abbas, and P. Rostalski, "A real-time gp based mpc for quadcopters with unknown disturbances," in *2022 American Control Conference (ACC)*, 2022, pp. 2051–2056.
- [7] I. Sa, M. Kamel, M. Burri, M. Bloesch, R. Khanna, P. Marija, J. Nieto, and R. Siegwart, "Build your own visual-inertial drone: A cost-effective and open-source autonomous drone," *IEEE Robotics & Automation Magazine*, vol. 25, no. 1, pp. 89–103, 2018.

- [8] Y. Sohège, M. Quiñones-Grueiro, and G. Provan, "A novel hybrid approach for fault-tolerant control of uavs based on robust reinforcement learning," in *2021 IEEE International Conference on Robotics and Automation (ICRA)*, 2021, pp. 10719–10725.
- [9] T. Johannink, S. Bahl, A. Nair, J. Luo, A. Kumar, M. Loskyll, J. A. Ojea, E. Solowjow, and S. Levine, "Residual reinforcement learning for robot control," in *2019 International Conference on Robotics and Automation (ICRA)*, 2019, pp. 6023–6029.
- [10] R. S. Sutton and A. G. Barto, *Reinforcement Learning: An Introduction*, 2nd ed. The MIT Press, 2018. [Online]. Available: <http://incompleteideas.net/book/the-book-2nd.html>
- [11] M. Taylor, S. Bashkirov, J. F. Rico, I. Toriyama, N. Miyada, H. Yanagisawa, and K. Ishizuka, "Learning bipedal robot locomotion from human movement," in *2021 IEEE International Conference on Robotics and Automation (ICRA)*, 2021, pp. 2797–2803.
- [12] Z. Li, X. Cheng, X. B. Peng, P. Abbeel, S. Levine, G. Berseth, and K. Sreenath, "Reinforcement learning for robust parameterized locomotion control of bipedal robots," in *2021 IEEE International Conference on Robotics and Automation (ICRA)*, 2021, pp. 2811–2817.
- [13] T. Miki, J. Lee, J. Hwangbo, L. Wellhausen, V. Koltun, and M. Hutter, "Learning robust perceptive locomotion for quadrupedal robots in the wild," *Science Robotics*, vol. 7, no. 62, p. eabk2822, 2022. [Online]. Available: <https://www.science.org/doi/abs/10.1126/scirobotics.abk2822>
- [14] D. Quillen, E. Jang, O. Nachum, C. Finn, J. Ibarz, and S. Levine, "Deep reinforcement learning for vision-based robotic grasping: A simulated comparative evaluation of off-policy methods," in *2018 IEEE International Conference on Robotics and Automation (ICRA)*, 2018, pp. 6284–6291.
- [15] M. B. Vankadari, K. Das, C. Shinde, and S. Kumar, "A reinforcement learning approach for autonomous control and landing of a quadrotor," in *2018 International Conference on Unmanned Aircraft Systems (ICUAS)*, 2018, pp. 676–683.
- [16] T. Haarnoja, A. Zhou, P. Abbeel, and S. Levine, "Soft actor-critic: Off-policy maximum entropy deep reinforcement learning with a stochastic actor," in *Proceedings of the 35th International Conference on Machine Learning*, ser. Proceedings of Machine Learning Research, J. Dy and A. Krause, Eds., vol. 80. PMLR, 10–15 Jul 2018, pp. 1861–1870. [Online]. Available: <https://proceedings.mlr.press/v80/haarnoja18b.html>
- [17] T. Haarnoja, A. Zhou, K. Hartikainen, G. Tucker, S. Ha, J. Tan, V. Kumar, H. Zhu, A. Gupta, P. Abbeel, and S. Levine, "Soft actor-critic algorithms and applications," *CoRR*, vol. abs/1812.05905, 2018. [Online]. Available: <http://arxiv.org/abs/1812.05905>
- [18] N. Koenig and A. Howard, "Design and use paradigms for gazebo, an open-source multi-robot simulator," in *IEEE/RSJ International Conference on Intelligent Robots and Systems*, Sendai, Japan, Sep 2004, pp. 2149–2154.
- [19] "AS-MC03-T English," <https://aerosense.co.jp/asmc03teng>, [Online; accessed 20-January-2023].
- [20] D. P. Kingma and J. Ba, "Adam: A method for stochastic optimization," in *3rd International Conference on Learning Representations, ICLR 2015, San Diego, CA, USA, May 7-9, 2015, Conference Track Proceedings*, Y. Bengio and Y. LeCun, Eds., 2015. [Online]. Available: <http://arxiv.org/abs/1412.6980>
- [21] "AS-MC03-W2 (in Japanese)," <https://aerosense.co.jp/products/drone/as-mc03-w2>, [Online; accessed 07-July-2023].
- [22] "Beaufort Wind Scale," <https://www.weather.gov/mfl/beaufort>, [Online; accessed 17-January-2023].